Research Article

Collapse versus Disruption: The Fate of Compact Self-Gravitating Systems in Ultralight Dark Matter Halos

Yuming Yang[1,2], Xiaojun Bi[1,2], Long Wang[3], Peng-Fei Yin[1]

1. State Key Laboratory of Particle Astrophysics, Chinese Academy of Sciences, Beijing, China; 2. School of Physical Sciences, University of Chinese Academy of Sciences, Beijing, China; 3. School of Physics and Astronomy, Sun Yat-Sen University, Guangzhou, China

Time-varying gravitational fluctuations induced by ultralight dark matter (ULDM) are expected to stochastically heat self-gravitating systems and drive them toward more diffuse configurations. Here we show that this intuition breaks down for sufficiently compact systems. We uncover a counterintuitive dynamical mechanism in which external heating can *accelerate*, rather than suppress, relaxation-driven core collapse. Using numerical simulations of compact stellar systems embedded in fluctuating backgrounds induced by ULDM, we find that their long-term evolution is governed by a nontrivial competition between two-body relaxation and stochastic heating, leading to distinct evolutionary outcomes, including core collapse, disruption, and quasi-stationary configurations. We further introduce a dimensionless parameter that quantifies the relative importance of relaxation and heating, which helps organize these regimes into a predictive phase diagram. Near the disruption boundary, we identify remnants with properties resembling those of ultra-faint dwarf galaxies. Our results reveal a previously unrecognized dynamical phase structure of self-gravitating systems in fluctuating gravitational backgrounds, with important implications for small-scale probes of ULDM.

Correspondence: papers@team.qeios.com — Qeios will forward to the authors

Introduction

Ultralight dark matter (ULDM) [1][2][3][4] forms halos with a distinctive wave-like structure, characterized by persistent density granules arising from field interference. The resulting fluctuations in the gravitational potential act as a source of dynamical heating for embedded stellar systems [5][6][7][8], and are traditionally expected to drive them toward more diffuse configurations and larger spatial extents [9]

 doi.org/10.32388/CFA66Q

[10][11][12][13][14][15]. Consequently, small-sized objects, such as nuclear star clusters [16][17][18] and ultra-faint dwarf galaxies (UFDs) [19][20], are often regarded as sensitive probes of the ULDM particle mass.

However, this conventional picture implicitly assumes that external heating dominates the long-term evolution. For sufficiently compact systems, internal two-body relaxation can proceed on timescales shorter than the age of the Universe [21][22], giving rise to phenomena such as core collapse and envelope expansion [21]. While relaxation-driven evolution is well understood in isolated star clusters [22][23], its interplay with ULDM fluctuations remains largely unexplored.

In this Letter, we study the evolution of compact systems within ULDM halos. Using a hybrid numerical framework that combines ULDM wave simulations [24] with direct N-body modeling of stellar dynamics [25], we find that the evolution is governed by a nontrivial competition between internal relaxation and ULDM-induced heating, leading to multiple distinct dynamical outcomes. Remarkably, in sufficiently dense systems, stochastic heating does not inhibit but instead accelerates relaxation-driven core collapse by preferentially stripping weakly bound outer stars, resulting in more centrally concentrated remnants. In contrast, initially more extended systems are dominated by heating and ultimately disrupted. Near the disruption boundary, we identify remnants whose properties resemble those of observed UFDs such as Segue 1 [26][27][28][29]. We further demonstrate that this competition organizes the long-term dynamics into three distinct evolutionary regimes, which are captured by a two-dimensional phase diagram.

Simulation setup

Owing to the large separation between the size of the stellar systems ($\lesssim 30$ pc) and the ULDM coherence length ($\sim$ kpc), the ULDM potential varies smoothly across the system, allowing its leading-order effect on the internal stellar dynamics (1) to be encoded in a time-dependent tidal tensor. We therefore adopt a two-stage framework in which the global ULDM dynamics and the internal stellar evolution are treated separately but consistently.

In the first stage, we exploit this scale separation by treating the stellar system as a mass point evolving within the ULDM halo, recording its trajectory and the associated ULDM-induced tidal tensor. The ULDM halo is evolved in an external tidal field motivated by Segue 1-like orbits [30], enabling a direct comparison with observations. To facilitate a controlled comparison among different stellar configurations, we perform a single first-stage simulation with a fiducial ULDM particle mass $m_a = 10^{-22} eV$ using the

PyUltraLight package [24] and apply the resulting tidal tensor to all second-stage simulations. Further details are provided in the Supplemental Material.

To sample the relevant region of parameter space, we consider six representative initial conditions. The stellar density profiles are taken to follow a Plummer profile [31] $\rho_\star(r) = (3M_\star/4\pi R_h^3)(1 + r^2/R_h^2)^{-5/2}$, with parameters chosen to span a range of compactness. Initial conditions are generated in approximate dynamical equilibrium using McLuster [32], and the adopted stellar masses $M_\star$, particle numbers N, and projected half-mass radii R_h are summarized in Tab. 1.

	S1	**S2**	**S3**	**S4**	**S5**	**S6**
$M_\star[10^3 M_\odot]$	1	1	5	100	100	25
$N[10^4]$	1	1	1	1	3	5
$R_h[pc]$	5	10	10	30	30	20

Table 1. Representative stellar systems used in this work.

In the second stage, we model the internal evolution of the stellar system using direct N-body simulations subject to the external tidal tensor extracted from the first stage. The corresponding ULDM-induced acceleration of a star at position $\mathbf{r}$ relative to the system's center of mass $\mathbf{r}_c$ can be approximated to leading order as

$$\Delta\mathbf{a}(\mathbf{r}, \mathbf{r}_c) \simeq -(\mathbf{r} - \mathbf{r}_c) \cdot \nabla\nabla V_{\rm ULDM}(\mathbf{r}_c), \tag{1}$$

where $\nabla\nabla V_{\rm ULDM}$ denotes the tidal tensor obtained from the first-stage simulation. These second-stage simulations are performed using PeTar [25], a high-accuracy direct N-body code appropriate for collisional stellar systems. For each initial condition, we carry out both a ULDM-influenced run and an isolated run without ULDM. Over the full simulation time of $13 Gyr$, the accumulated energy error in all isolated runs remains below 0.015%, ensuring that numerical artifacts do not affect our conclusions. In the ULDM-influenced simulations, the system's center of mass is fixed at $\mathbf{r}_c = \mathbf{0}$, and the ULDM-induced acceleration is incorporated through Eq. 1 for each stellar particle.

Fig. 1 illustrates the temporal evolution of the projected stellar density profiles and velocity dispersions for the six representative systems. Solid and dashed curves denote systems evolving in ULDM halos and in isolation, respectively, while different colors correspond to different evolutionary times.

Stellar dynamics without ULDM

In isolation, sufficiently compact stellar systems undergo relaxation-driven core collapse. This evolution is characterized by a progressive increase of the central density and a contraction of the core, accompanied by an expansion of the outer envelope. These features are illustrated by system S1 (dashed curves in the first panel of Fig. 1) and by the corresponding evolution of the projected surface density in Fig. 2. The core radius (defined as in [33]) and Lagrangian radii [(2)] (dashed curves in Fig. 3) exhibit the canonical signatures of this process: monotonic central contraction and envelope expansion (e.g., increasing $r_{0.9}$) driven by outward energy transport through two-body encounters.

The isolated evolution is governed by two-body relaxation on a characteristic timescale [34], $t_r = 0.065\langle v^2\rangle^{3/2}/(\rho\langle m\rangle G^2 \ln\Lambda)$, where $\langle m\rangle$ is the mean stellar mass, $\ln\Lambda \sim \ln N$ is the Coulomb logarithm, and $\langle v^2\rangle$ and ρ denote the local mean-squared velocity and density, respectively. For the global evolution of the system, the relevant timescale is the half-mass relaxation time [22][34],

$$t_{rh} = 0.138\frac{M_\star r_h^{3/2}}{\langle m\rangle G^{1/2}\ln\Lambda} \simeq \frac{0.212 N R_h^{3/2}}{M_\star G^{1/2}\ln\Lambda}, \tag{2}$$

where r_h is the three-dimensional half-mass radius, related to the projected half-mass radius by $r_h \simeq (4/3)R_h$ under the assumption of spherical symmetry [29].

The parameter dependences implied by Eq. 2 are borne out by the isolated evolution of all our systems (dashed curves in Fig. 1). For instance, S2 differs from S1 only by a larger initial size R_h and therefore undergoes a slower collapse. Conversely, the larger total stellar mass $M_\star$ of S3 leads to a more rapid and pronounced contraction, while the larger particle number N in S5 compared to S4 results in a slower overall evolution. Taken together, these trends establish two-body relaxation as the sole driver of the isolated dynamics and provide a controlled baseline for isolating the impact of ULDM-induced fluctuations discussed below.

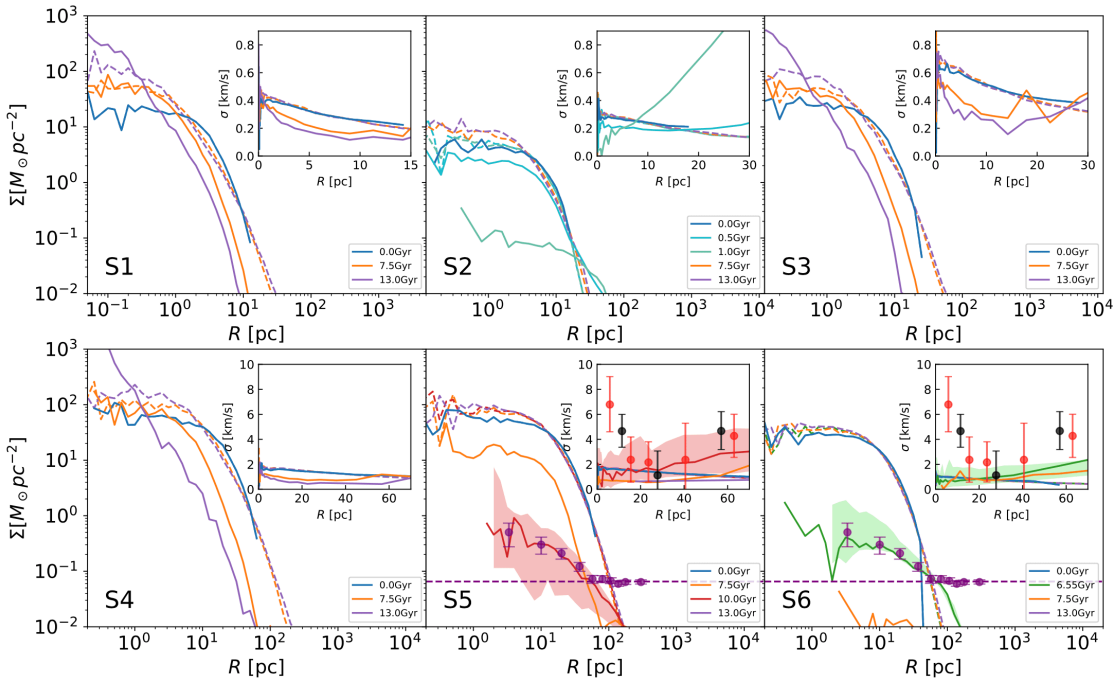

Figure 1. Circularly averaged stellar surface density profiles projected along the z-direction (main panels) and corresponding z-direction velocity dispersion profiles (insets) for the six simulated systems at different evolutionary times. Colors indicate time, while solid and dashed curves denote evolution with and without ULDM, respectively. Shaded regions in the last two panels show the scatter over 100 random viewing directions. Observational data for Segue 1 are overplotted: stellar surface density from [27] (purple points) and line-of-sight velocity dispersions from [28] (red and black points, corresponding to bins of 15 and 23 stars). The surface density profile is normalized to a total stellar mass of $\sim 800 M_\odot$, consistent with observational uncertainties.

Accelerated core collapse

At first glance, relaxation-driven core collapse, which makes stellar systems more centrally concentrated, and ULDM-induced heating, which tends to puff them up, are expected to counteract each other. One would therefore anticipate that external heating generally suppresses or delays collapse. Contrary to this expectation, we find that in sufficiently compact systems, ULDM heating can instead accelerate core collapse.

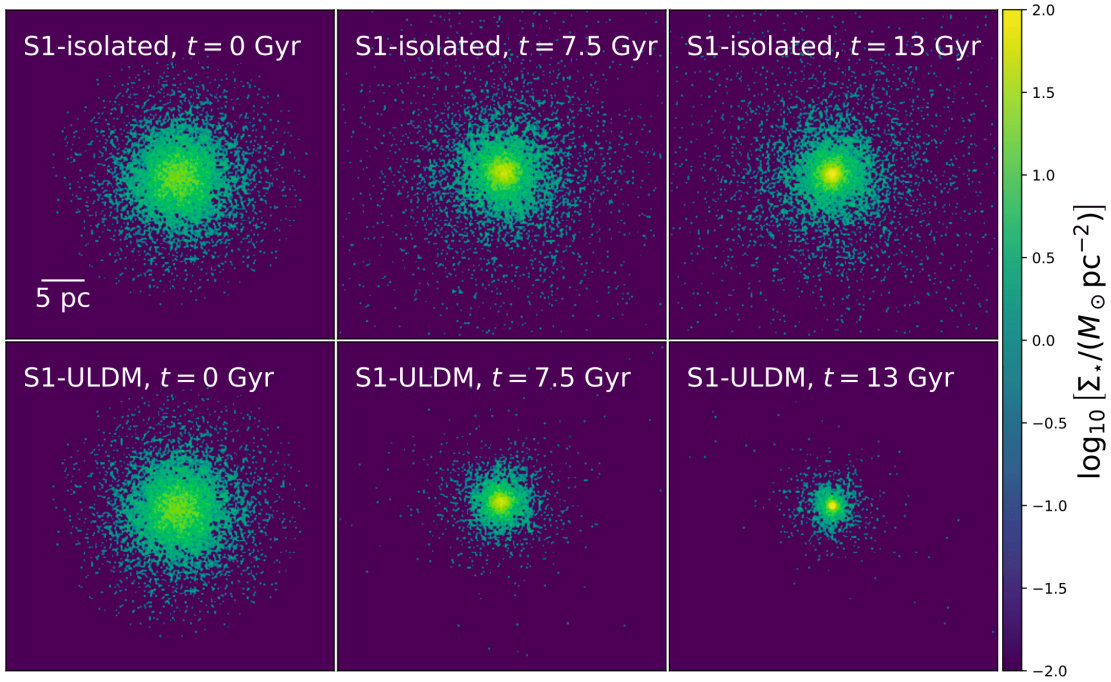

Figure 2. Stellar surface density maps of system S1 at different evolutionary times, projected along the z-direction. The upper and lower rows show evolution without and with ULDM, respectively.

This behavior is evident in systems S1, S3, and S4, which lie in the collapse-dominated regime. In these cases, the ULDM-influenced evolution (solid curves) exhibits a systematically faster increase of the central density and a more rapid contraction of the core than in isolation (dashed curves), as shown in Fig. 1. The projected surface density maps of S1 (Fig. 2) further illustrate this behavior: ULDM-induced fluctuations preferentially strip weakly bound stars from the outskirts, leaving behind a remnant that is more centrally concentrated than its isolated counterpart after 13 Gyr. Consistently, the core radius in the presence of ULDM contracts significantly faster than in isolation, as seen from the comparison of the red solid and dashed curves in Fig. 3.

This counterintuitive acceleration of collapse admits a simple physical explanation. From Eq. (2), ULDM heating reduces the bound stellar mass, thereby shortening the global relaxation timescale. Alternatively, heating-induced mass loss lowers the depth of the stellar potential, leading to a reduction of the velocity dispersion σ (inset of the first panel of Fig. 1). Through the dependence of the local relaxation time t_r on $v^2 \simeq 3\sigma^2$, this reduction enhances two-body relaxation. As a result, the characteristic relaxation time in the inner regions drops substantially; for S1, the averaged relaxation time within $r_{0.05}$ decreases to

doi.org/10.32388/CFA66Q

$\sim 25\%$ of its isolated value by the end of the evolution (inset of Fig. 3). From a thermodynamic perspective, ULDM-induced stripping steepens the radial gradient of the velocity dispersion (inset of the first panel of Fig. 1), effectively increasing the temperature contrast between the inner and outer regions. This enhances the outward transport of energy and naturally drives a more rapid gravothermal contraction of the core, analogous to self-interacting dark matter core collapse [35][36].

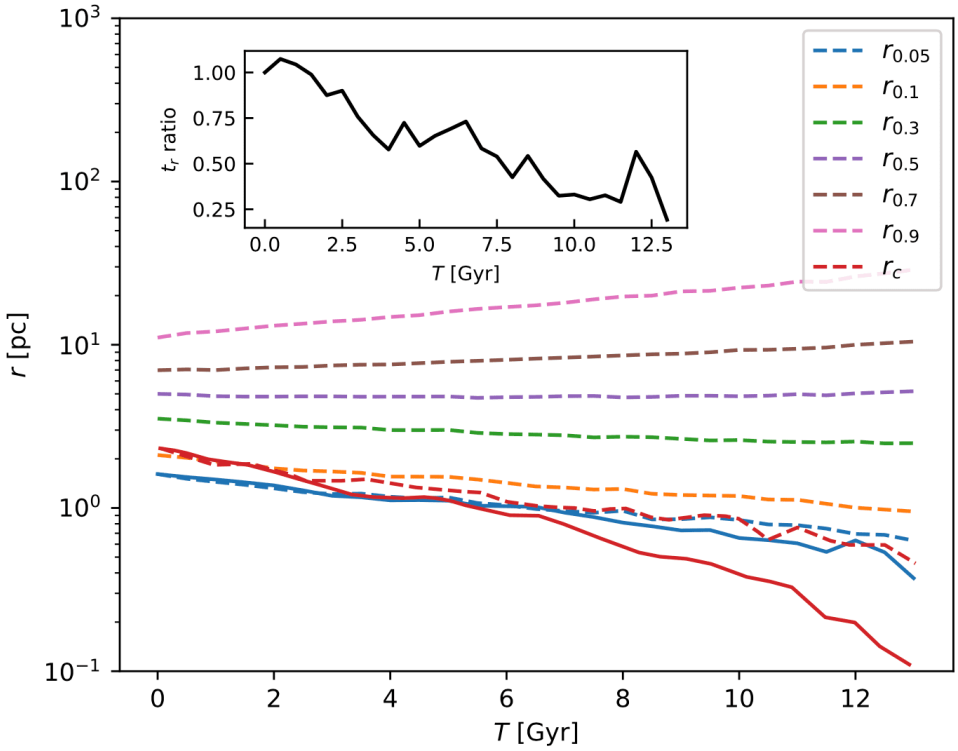

Figure 3. Time evolution of the core radius r_c and Lagrangian radii of S1, color-coded by enclosed mass fraction. Solid and dashed curves show the evolution with and without ULDM, respectively. The inset displays the ratio of the relaxation time averaged within $r_{0.05}$ between the ULDM-influenced and isolated cases, illustrating the ULDM-induced shortening of the inner relaxation timescale.

Heating-dominated disruption

As the initial stellar distribution becomes more diffuse, ULDM-induced heating increasingly dominates the evolution and, beyond a critical threshold, leads to complete disruption.

This behavior is illustrated by the contrast between S1 and S2, which share the same total stellar mass and particle number but differ in their initial half-mass radii. As shown in the second panel of Fig. 1, the more extended system S2 undergoes rapid expansion and becomes nearly unbound within ~ 1 Gyr. Meanwhile, the velocity dispersion rises sharply, reflecting the continuous injection of energy by ULDM fluctuations and the transition from a self-gravitating configuration to a dispersing state. This transition reflects two generic effects: first, the lower initial density of more extended systems weakens their self-gravity relative to the ULDM background; second, relaxation becomes inefficient owing to the scaling $t_{rh} \propto R_h^{3/2}$, allowing external heating to dominate the long-term evolution. Consistently, increasing the stellar mass by a factor of five, as in S3, restores relaxation dominance and leads back to collapse-driven behavior (third panel of Fig. 1).

A similar competition is seen in the comparison between S4 and S5, which share the same smooth density profile but differ in particle number. The stronger two-body relaxation in S4 enables core collapse, with ULDM fluctuations further accelerating the contraction while preserving overall stability. In contrast, the weaker relaxation in S5 allows heating to prevail, driving the system close to disruption by $\sim 10Gyr$. This comparison shows that, even for identical smooth density profiles, variations in relaxation efficiency alone can qualitatively change the evolutionary fate.

Near disruption: Segue 1-analog system

Near the disruption boundary, ULDM-heated systems develop structural and kinematic properties that resemble those of observed UFDs [26], [29]. As a representative example, we compare our simulations with the UFD Segue 1, whose stellar surface density [27] and line-of-sight velocity dispersion [28] profiles are shown in the last two panels of Fig. 1.

At $t \simeq 10Gyr$, system S5 approaches the disruption threshold and exhibits projected profiles broadly consistent with the observations (red solid curves). The remaining bound population is small (~ 400 stars within 60 pc), so projections along 100 random lines of sight display substantial scatter (shaded regions), naturally encompassing the observed data. The steep central rise in the measured velocity dispersion may point to additional physics not included here, such as the presence of a compact central object [37].

Although the particle mass in S5 ($\sim 3.3M_\odot$) is not representative of a realistic stellar mass spectrum [38], we have verified that Segue 1-like systems can also be obtained with more realistic masses. In particular, system S6, with particle mass of $0.5M_\odot$, reproduces similar surface density and velocity dispersion profiles at $t \simeq 6.55Gyr$ (last panel of Fig. 1), albeit at a younger age.

Overall, our results suggest that for a ULDM particle mass of $10^{-22}eV$, Segue 1 can be interpreted as a system observed near disruption [15]. Our aim here is not to provide an exact evolution scenario for specific UFDs, but to demonstrate that ULDM-induced heating, when combined with internal relaxation, can give rise to a broad family of evolutionary pathways, among which UFD-like remnants emerge as a generic outcome. Incorporating additional physics, such as a realistic stellar initial mass function [38], binaries [39][40], and stellar evolution [40], will further enrich this landscape and expand the range of attainable morphologies.

Phase diagram

The long-term evolution of compact stellar systems in ULDM halos is organized into three distinct dynamical regimes, controlled by the relaxation timescale t_{rh}, the ULDM-driven disruption timescale $t_{dis} = (3M_\star/4\pi\bar{\rho}_{ULDM}R_h^3)(\lambda_{dB}/\sigma_{ULDM})$ [3], for which we adopt the phenomenological estimate of Ref. [15] in the regime $R_h \ll \lambda_{dB}$, and their ratio

$$\alpha \equiv \frac{t_{rh}}{t_{dis}} = 0.153 \left(\frac{N}{10^4}\frac{4}{\lg N}\right)\left(\frac{10^3 M_\odot}{M_\star}\right)^{3/2}\left(\frac{R_h}{10pc}\right)^{9/2} \times\left(\frac{m_a c^2}{10^{-22}eV}\right)\left(\frac{\bar{\rho}_{ULDM}}{3.18\times10^6 M_\odot kpc^{-3}}\right)\left(\frac{\sigma_{ULDM}}{20kms^{-1}}\right)^2, \tag{3}$$

with larger α indicating increasing dominance of ULDM heating. Extensive simulations reveal three characteristic thresholds: for $t_{rh} \gtrsim 4.7Gyr$ ($t_{dis} \gtrsim 85.0Gyr$), relaxation (heating) remains dynamically irrelevant over the age of the Universe ($\sim 13Gyr$), while a critical ratio $\alpha \simeq 0.05$ separates heating-dominated from relaxation-dominated evolution for moderate N. We emphasize that, in this sense, t_{rh} and t_{dis} act as characteristic timescale parameters rather than sharp transition points, with the simulated onset of collapse or disruption differing by factors of order unity.

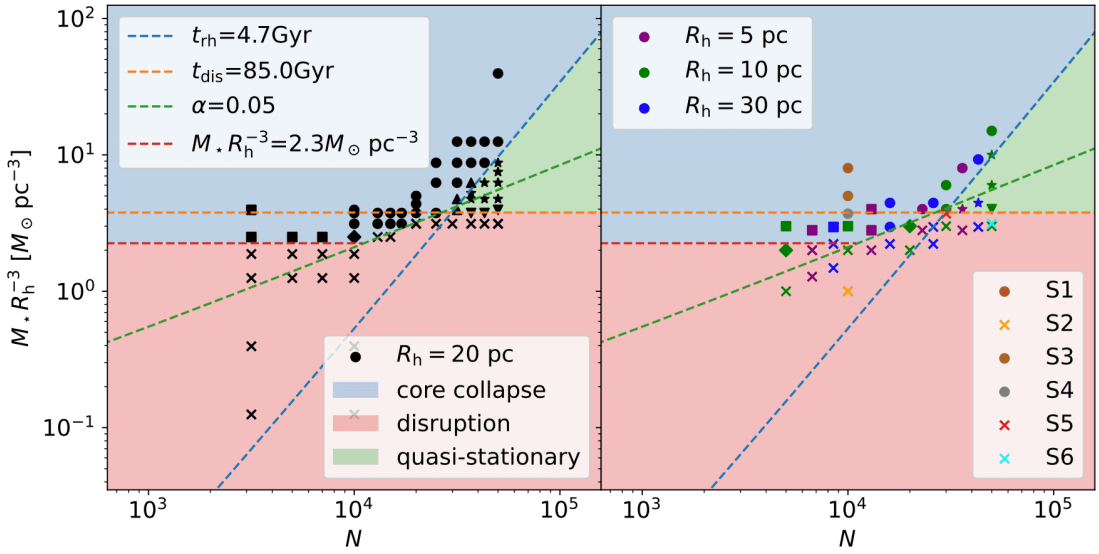

Figure 4. Phase diagram of stellar systems within a ULDM halo with $m_a = 10^{-22}$eV. Filled circles, crosses, and pentagrams denote systems undergoing core collapse, disruption, and quasi-stationary evolution, respectively. Squares mark systems with strong collapse that are susceptible to numerical artifacts. Upward triangles, downward triangles, and diamonds indicate intermediate cases between collapse and quasi-stationary, disruption and quasi-stationary, and collapse and disruption, respectively, and are therefore difficult to classify unambiguously. Colors encode different R_h. The six simulation sets S1-S6 are indicated separately.

Remarkably, stellar systems with different initial parameters $(M_\star, N, R_h)$ can be mapped onto a single plane spanned by $(N, M_\star R_h^{-3})$ (Fig. 4), reflecting the degeneracy between $M_\star$ and R_h implied by the analytic scalings of t_{rh}, t_{dis}, and α. Moreover, the three thresholds introduced above partition this plane into three well-defined dynamical phases: a relaxation-dominated phase characterized by core collapse, a heating-dominated phase leading to disruption, and a quasi-stationary phase in which neither process operates efficiently. A small subset of the heating-dominated region lies at $\alpha < 0.05$, where extremely low stellar densities cause any partial core contraction to be ultimately overwhelmed by ULDM-driven mass loss. The simulated evolutionary outcomes, marked by different symbols, populate well-separated regions of this phase diagram, demonstrating the predictive power of this classification.

The near-intersection of the three phase boundaries is not coincidental. At the intersection of the t_{rh} and t_{dis} boundaries, both relaxation and heating become relevant at $\sim 13Gyr$. As a result, the two effects are comparable at this point, and it therefore naturally lies on the critical α boundary. This convergence further demonstrates the consistency between the analytic scalings and the simulations.

Taken together, this phase diagram provides a unified and predictive framework for understanding the fate of compact stellar systems in ULDM halos, revealing that their long-term evolution is organized into distinct dynamical phases. Finally, we emphasize that the above analysis is performed at fixed ULDM particle mass, halo, and orbital parameters, and therefore isolates the dependence on the initial stellar system properties. Whether the scalings with these former quantities follow Eq. 3 remains to be explored.

Conclusions

We have demonstrated that the evolution of compact stellar systems embedded in ULDM halos is governed by a nontrivial competition between internal relaxation and wave-induced heating. Contrary to naive expectations, ULDM-driven heating does not generically suppress gravitational collapse; instead, in sufficiently compact systems, it can accelerate relaxation-driven core collapse. This competition organizes the long-term dynamics into three distinct evolutionary regimes, encapsulated in a single phase diagram. This classification provides a predictive framework for assessing the fate of stellar systems in ULDM halos. Our results establish compact stellar systems as sensitive dynamical probes of ULDM and open a new pathway for confronting ULDM models with observations.

Statements and Declarations

Acknowledgements

We thank Shuo Li and Hui Li for useful discussions. This work is supported by the National Natural Science Foundation of China under grants No.12447105, No.12575113, No.12573041, and No.12233013. L.W. thanks the High-level Youth Talent Project (Provincial Financial Allocation) through the grant 2023HYSPT0706, the Fundamental Research Funds for the Central Universities, Sun Yat-sen University (2025QNPY04).

Footnotes

[1] This effect has two physically distinct contributions. One originates from the intrinsic wave interference of ULDM, which generates time-dependent fluctuations in the gravitational field and induces stochastic dynamical heating. The other arises from tidal forces associated with spatial gradients of the smooth, time-averaged ULDM potential when the stellar system is displaced from the halo center. Our simulations

incorporate both effects self-consistently, and we collectively refer to their combined impact as ULDM-induced heating.

[2] The Lagrangian radii denote the three-dimensional radii enclosing fixed fractions of the total stellar mass.

[3] Since the stellar system undergoes bounded orbital motion within a region of characteristic size $r_{\rm orbit} \simeq 3\,{\rm kpc}$ around the halo center (see Supplemental Material), the mean ULDM density is taken to be $\bar{\rho}_{\rm ULDM} = 3M_{\rm ULDM}(< r_{\rm orbit})/4\pi r_{\rm orbit}^3$.

References

1. ^Hu W, Barkana R, Gruzinov A (2000). "Fuzzy Cold Dark Matter: The Wave Properties of Ultralight Particles." Phys Rev Lett. **85**(6):1158–1161. doi:10.1103/physrevlett.85.1158.
2. ^Peebles PJE (2000). "Fluid Dark Matter." Astrophys J. **534**(2):L127–L129. doi:10.1086/312677.
3. ^Hui L, Ostriker JP, Tremaine S, Witten E (2017). "Ultralight Scalars as Cosmological Dark Matter." Phys Rev D. **95**(4). doi:10.1103/physrevd.95.043541.
4. ^Hui L (2021). "Wave Dark Matter." Annu Rev Astron Astrophys. **59**(1):247–289. doi:10.1146/annurev-astro-120920-010024.
5. ^Bar-Or B, Fouvry J, Tremaine S (2019). "Relaxation in a Fuzzy Dark Matter Halo." Astrophys J. **871**(1):28. doi:10.3847/1538-4357/aaf28c.
6. ^El-Zant AA, Freundlich J, Combes F, Halle A (2019). "The Effect of Fluctuating Fuzzy Axion Haloes on Stellar Dynamics: A Stochastic Model." Mon Not R Astron Soc. **492**(1):877–894. doi:10.1093/mnras/stz3478.
7. ^Church BV, Mocz P, Ostriker JP (2019). "Heating of Milky Way Disc Stars by Dark Matter Fluctuations in Cold Dark Matter and Fuzzy Dark Matter Paradigms." Mon Not R Astron Soc. **485**(2):2861–2876. doi:10.1093/mnras/stz534.
8. ^Chiang BT, Ostriker JP, Schive HY (2023). "Can Ultralight Dark Matter Explain the Age–Velocity Dispersion Relation of the Milky Way Disc: A Revised and Improved Treatment." Mon Not R Astron Soc. **518**(3):4045–4063. doi:10.1093/mnras/stac3358.
9. ^Dutta Chowdhury D, van den Bosch FC, van Dokkum P, Robles VH, Schive HY, Chiueh T (2023). "On the Dynamical Heating of Dwarf Galaxies in a Fuzzy Dark Matter Halo." Astrophys J. **949**(2):68. doi:10.3847/1538-4357/acc73d.

10. ^Teodori L, Caputo A, Blum K (2025). "Ultra-Light Dark Matter Simulations and Stellar Dynamics: Tension in Dwarf Galaxies for $m < {5 \times 10^{- 21}}$ eV."

11. ^Zhao Y, Benson A, Du X (2025). "A Semi-Analytic Model for Effects of Fuzzy Dark Matter Granule Perturbations on Orbital Motion." https://arxiv.org/abs/2507.07963.

12. ^Yang YM, Bi XJ, Yin PF (2024). "A Theoretical Perspective on the Almost Dark Galaxy Nube: Exploring the Fuzzy Dark Matter Model." J Cosmol Astropart Phys. **2024**(07):054. doi:10.1088/1475-7516/2024/07/054.

13. ^Yang YM, Zhang ZC, Bi XJ, Yin PF (2025). "Interpreting the Extremely Diffuse Stellar Distribution of the Nube Galaxy through Fuzzy Dark Matter." Astrophys J Lett. **981**(2):L26. doi:10.3847/2041-8213/adb7da.

14. ^Yang YM, Zhang ZC, Bi XJ, Yin PF (2025). "Tidal Suppression of Fuzzy Dark Matter Heating in Milky Way Satellite Galaxies." Astrophys J Lett. **990**(2):L67. doi:10.3847/2041-8213/adff81.

15. a, b, cEberhardt A, Gosenca M, Hui L (2025). "Heating and Scattering of Stellar Distributions by Ultralight Dark Matter."

16. ^Marsh DJE, Niemeyer JC (2019). "Strong Constraints on Fuzzy Dark Matter from Ultrafaint Dwarf Galaxy Eridanus II." Phys Rev Lett. **123**(5):051103. doi:10.1103/physrevlett.123.051103.

17. ^Schive HY, Chiueh T, Broadhurst T (2020). "Soliton Random Walk and the Cluster-Stripping Problem in Ultralight Dark Matter." Phys Rev Lett. **124**(20):201301. doi:10.1103/physrevlett.124.201301.

18. ^Chiang BT, Schive HY, Chiueh T (2021). "Soliton Oscillations and Revised Constraints from Eridanus II of Fuzzy Dark Matter." Phys Rev D. **103**(10):103019. doi:10.1103/physrevd.103.103019.

19. ^Dalal N, Kravtsov A (2022). "Excluding Fuzzy Dark Matter with Sizes and Stellar Kinematics of Ultrafaint Dwarf Galaxies." Phys Rev D. **106**(6):063517. doi:10.1103/physrevd.106.063517.

20. ^May S, Dalal N, Kravtsov A (2025). "Updated Bounds on Ultra-Light Dark Matter from the Tiniest Galaxies."

21. a, bBinney J, Tremaine S (2008). Galactic Dynamics: Second Edition.

22. a, b, cMeylan G, Heggie DC (1997). "Internal Dynamics of Globular Clusters." Astron Astrophys Rev. **8**(1–2):1–143. doi:10.1007/s001590050008.

23. ^Wang L, Spurzem R, Aarseth S, Giersz M, Askar A, Berczik P, Naab T, Schadow R, Kouwenhoven MBN (2016). "The Dragon Simulations: Globular Cluster Evolution with a Million Stars." Mon Not R Astron Soc. **458**(2):1450–1465. doi:10.1093/mnras/stw274.

24. a, bEdwards F, Kendall E, Hotchkiss S, Easther R (2018). "PyUltraLight: A Pseudo-Spectral Solver for Ultralight Dark Matter Dynamics." J Cosmol Astropart Phys. **2018**(10):027–027. doi:10.1088/1475-7516/2018/10/027.

25. a, bWang L, Iwasawa M, Nitadori K, Makino J (2020). "Petar: A High-Performance N-Body Code for Modelling Massive Collisional Stellar Systems." Mon Not R Astron Soc. **497**(1):536–555. doi:10.1093/mnras/staa1915.

26. ^ a, b *Belokurov V, Zucker DB, Evans NW, Kleyna JT, Koposov S, Hodgkin ST, Irwin MJ, Gilmore G, Wilkinson MI, Fellhauer M, Bramich DM, Hewett PC, Vidrih S, De Jong JTA, Smith JA, Rix HW, Bell EF, Wyse RFG, Newberg H J, Mayeur PA, Yanny B, Rockosi CM, Gnedin OY, Schneider DP, Beers TC, Barentine JC, Brewington H, Brinkma nn J, Harvanek M, Kleinman SJ, Krzesinski J, Long D, Nitta A, Snedden SA (2007). "Cats and Dogs, Hair and a Hero: A Quintet of New Milky Way Companions." Astrophys J.* ***654****(2):897–906. doi:10.1086/509718.*

27. ^ a, b, c *Martin NF, de Jong JTA, Rix HW (2008). "A Comprehensive Maximum Likelihood Analysis of the Structu ral Properties of Faint Milky Way Satellites." Astrophys J.* ***684****(2):1075–1092. doi:10.1086/590336.*

28. ^ a, b, c *Simon JD, Geha M, Minor QE, Martinez GD, Kirby EN, Bullock JS, Kaplinghat M, Strigari LE, Willman B, C hoi PI, Tollerud EJ, Wolf J (2011). "A Complete Spectroscopic Survey of the Milky Way Satellite Segue 1: The Da rkest Galaxy." Astrophys J.* ***733****(1):46. doi:10.1088/0004-637x/733/1/46.*

29. ^ a, b, c *Simon JD (2019). "The Faintest Dwarf Galaxies." Annu Rev Astron Astrophys.* ***57****(1):375–415. doi:10.1146/ annurev-astro-091918-104453.*

30. ^ *Pace AB, Erkal D, Li TS (2022). "Proper Motions, Orbits, and Tidal Influences of Milky Way Dwarf Spheroida l Galaxies." Astrophys J.* ***940****(2):136. doi:10.3847/1538-4357/ac997b.*

31. ^ *Plummer HC (1911). "On the Problem of Distribution in Globular Star Clusters: (Plate 8.)." Mon Not R Astron Soc.* ***71****:460–470. doi:10.1093/mnras/71.5.460.*

32. ^ *Küpper AHW, Maschberger T, Kroupa P, Baumgardt H (2011). "Mass Segregation and Fractal Substructure i n Young Massive Clusters - I. The McLuster Code and Method Calibration." Mon Not R Astron Soc.* ***417****(3):230 0–2317. doi:10.1111/j.1365-2966.2011.19412.x.*

33. ^ *Casertano S, Hut P (1985). "Core Radius and Density Measurements in N-Body Experiments Connections wi th Theoretical and Observational Definitions." Astrophys J.* ***298****:80–94. doi:10.1086/163589.*

34. ^ a, b *Spitzer L (1987). Dynamical Evolution of Globular Clusters.*

35. ^ *Sameie O, Yu HB, Sales LV, Vogelsberger M, Zavala J (2020). "Self-Interacting Dark Matter Subhalos in the M ilky Way's Tides." Phys Rev Lett.* ***124****(14). doi:10.1103/physrevlett.124.141102.*

36. ^ *Nishikawa H, Boddy KK, Kaplinghat M (2020). "Accelerated Core Collapse in Tidally Stripped Self-Interacti ng Dark Matter Halos." Phys Rev D.* ***101****(6). doi:10.1103/physrevd.101.063009.*

37. ^ *Lujan N, Gebhardt K, Anantua R, Chase O, Debski MH, Finley C, Gomez LV, Gupta O, Lawson AJ, Marron I, M artinez Z, Painter CA, Sklansky Y, West H (2025). "Modeling the "Dark-Matter Dominated" Dwarf Galaxy Seg ue 1 with a Supermassive Black Hole." Astrophys J Lett.* ***992****(2):L25. doi:10.3847/2041-8213/ae0b4f.*

38. ^ a, b *Kroupa P (2002). "The Initial Mass Function of Stars: Evidence for Uniformity in Variable Systems." Scien ce.* ***295****(5552):82–91. doi:10.1126/science.1067524.*

39. ^Pianta C, Capuzzo-Dolcetta R, Carraro G (2022). "The Impact of Binaries on the Dynamical Mass Estimate of Dwarf Galaxies." Astrophys J. **939**(1):3. doi:10.3847/1538-4357/ac9303.

40. a, bFlammini Dotti F, Capuzzo-Dolcetta R, Carraro G, Trani AA, Spurzem R (2026). "The Long-Term Evolution of Ultra Faint Dwarf Galaxies and Observational Implications." https://arxiv.org/abs/2601.13049.

Supplementary data: available at https://doi.org/10.32388/CFA66Q

Declarations

Funding: National Natural Science Foundation of China under grants No.12447105, No.12575113, No.12573041, and No.12233013

Potential competing interests: No potential competing interests to declare.